JACS
JOURNAL OF THE AMERICAN CHEMICAL SOCIETY
Communication
pubs.acs.org/JACS

A Luminescent and Biocompatible PhotoCORM†

Agustin E. Pierri, Alessia Pallaoro, Guang Wu, and Peter C. Ford*

Department of Chemistry and Biochemistry, University of California, Santa Barbara, California 93106, United States

Supporting Information

ABSTRACT: The water-soluble rhenium(I) complex *fac*-$[Re(bpy)(CO)_3(thp)]^+$ (**1**) [$CF_3SO_3^-$ salt; bpy = 2,2′-bipyridine, thp = tris(hydroxymethyl)phosphine] is both strongly luminescent and photoactive toward carbon monoxide release. It is stable in aerated aqueous media, is incorporated into cells from the human prostatic carcinoma cell line PPC-1, and shows no apparent cytotoxicity. Furthermore, the solvated Re(I) photoproduct of CO release (**2**) is also luminescent, a feature that allows one to track the transformation of **1** to **2** inside such cells using confocal fluorescence microscopy. In this context, **1** is a very promising candidate as a photoactivated CO releasing moiety (photoCORM) with potential therapeutic applications.

Although long known as a gas that is toxic to humans, carbon monoxide is formed endogenously during the catabolism of hemes by the enzyme heme oxygenase.[1] Over the past decade, various studies have implicated roles of CO in wound healing and cardiovascular protection.[2] Additionally, exogenous application of CO has been linked to improved proliferation of vascular smooth muscle cells, reduced organ graft rejection, and protection against ischemia/reperfusion injury.[3] Thus, as for the bioactive small molecules NO and H_2S,[4] the evolving understanding of CO physiology has led to greater appreciation of the potential therapeutic value of targeted CO delivery.[5] Current methods include mixing CO with breathing air as well as using CO-releasing moieties (CORMs) based on transition metals or boron.[6] However, these approaches suffer from a lack of target selectivity and dosage control. To combat these shortcomings, we and others have initiated investigations of photochemical CO delivery.[7] Photolysis-induced release of caged[8] CO has the potential to provide exceptional control over location, timing, and dosage, since the command signal would be the absorption of light. The photoactive CORM (photoCORM) precursors serve as benign CO reservoirs that are triggered upon irradiation. However, a crucial challenge is to assess the location and extent of CO release in vivo. To address this issue, we describe here a novel photoCORM that, in addition to releasing CO, can serve as a luminescent indicator for the location and extent of intracellular photochemical CO release.

Complexes of the type *fac*-$[Re(bpy)(CO)_3(X)]$ (bpy = 2,2′ bipyridine; X = Cl, Br) are well-known as CO oxidation catalysts and as relatively photoinert luminophores.[9] However, Ishitani and co-workers have shown that replacing the halide with a π-acid makes the axial CO photolabile.[10] Indeed, the cationic complexes $[Re(bpy)(CO)_3(PR_3)]^+$ (R = Ph, ^{i}Pr, Me, O^{i}Pr, OMe) undergo photodissociation of one CO upon irradiation in the near-UV, but these materials are only marginally water-soluble. To address this issue, we prepared the uncharged but water-soluble phosphine ligand tris-

Scheme 1. Synthetic Scheme for the Preparation of *fac*-$[Re(bpy)(CO)_3(L)](CF_3SO_3)$ [L = $P(CH_2OH)_3$]

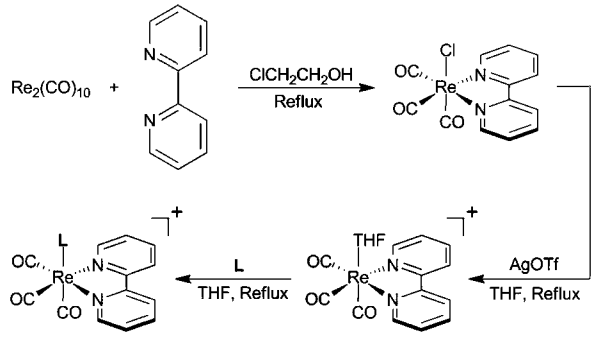

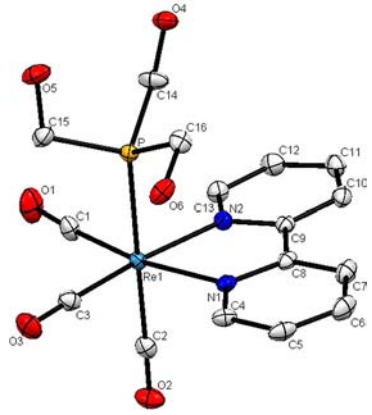

Figure 1. Molecular structure of *fac*-$[Re(bpy)(CO)_3(thp)]^+$ (**1**), shown with thermal ellipsoids at 50% probability. H atoms and the $CF_3SO_3^-$ counterion have been omitted for clarity. Selected bond lengths (Å) and angles (deg): Re1−C1, 1.9164(2); Re1−C2, 1.9685(1); Re1−C3, 1.9270(2); Re1−P1, 2.4478(4); P1−Re1−C1, 88.44(5); P1−Re1−C2, 179.25(4); P1−Re1−C3 , 90.90(4).

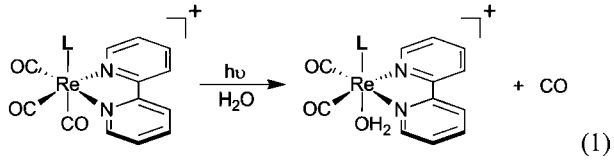

(1)

Received: August 24, 2012
Published: October 18, 2012

   dx.doi.org/10.1021/ja3084434 | J. Am. Chem. Soc. 2012, 134, 18197−18200

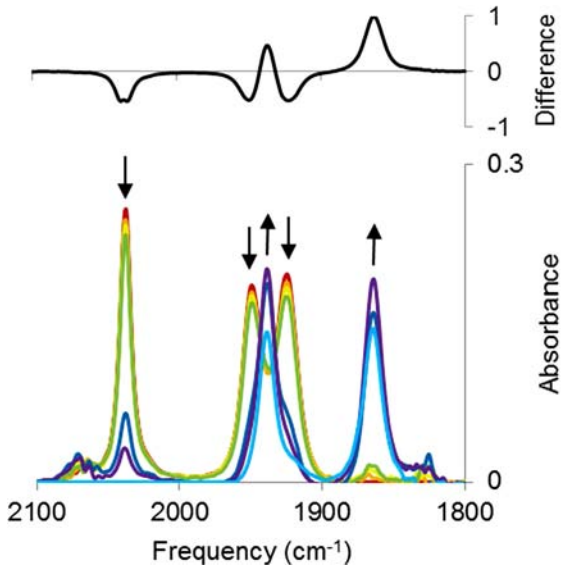

Figure 2. Bottom: FTIR spectrum (ν_{CO} region) of the triflate salt of **1** in acetonitrile solution and the changes that occur during 405 nm photolysis. Top: Difference spectrum between **1** and the photoproduct **2**. The disappearance of the bands at 2037, 1949, and 1923 cm^{-1} and the growth of two new bands at 1937 and 1862 cm^{-1} suggest the loss of a single CO.

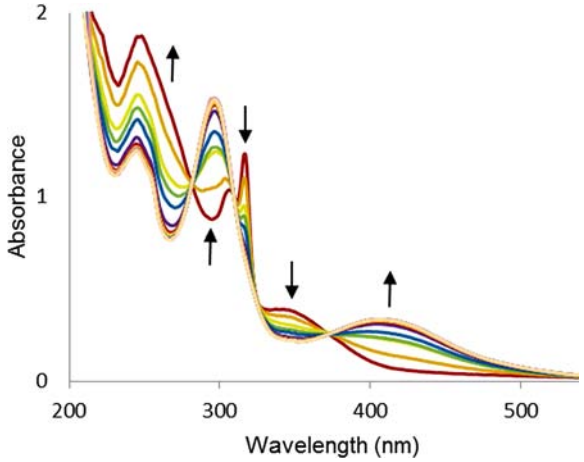

Figure 3. Optical spectral changes during 405 nm photolysis of **1** in PBS at 37 °C. The red shift of the MLCT band from 345 to 405 nm is characteristic of a loss of CO from the metal center.

(hydroxymethyl)phosphine (thp) from tetrakis-(hydroxymethyl)phosphonium chloride according to a modified version of a literature procedure[11] [see the Supporting Information (SI)]. The complex *fac*-$[Re(bpy)(CO)_3(thp)]^+$ (**1**, triflate salt) was then synthesized by modified literature procedures according to Scheme 1 (see the SI for details).

The solid-state X-ray crystal structure of the triflate salt of **1** (Figure 1) shows Re1−C2 bond elongation [1.968 Å vs 1.922 Å (average) for Re1−C1 and Re1−C3] due to the π-acidity of the trans phosphine (see the SI). The positive-ion-mode electrospray ionization mass spectrum showed peaks at m/z 551.04 $[M]^+$ and m/z 523.04 $[M - CO]^+$. The IR spectrum of an acetonitrile solution of the triflate salt of **1** displayed three ν_{CO} bands at 2037, 1949, and 1923 cm^{-1} (Figure 2), consistent with the C_s symmetry of this cation. The electronic absorption spectrum displayed a metal-to-ligand charge transfer (MLCT)

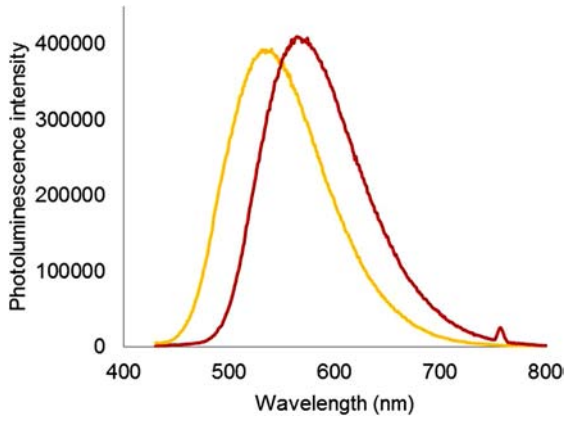

Figure 4. Emission spectra of **1** (yellow) and **2** (red) in phosphate buffer (10 mM, pH 7.4). The luminescence from **2** was recorded after exhaustive photolysis (λ_{ex} = 405 nm) of a solution initially containing the CF_3SO_3 salt of **1**.

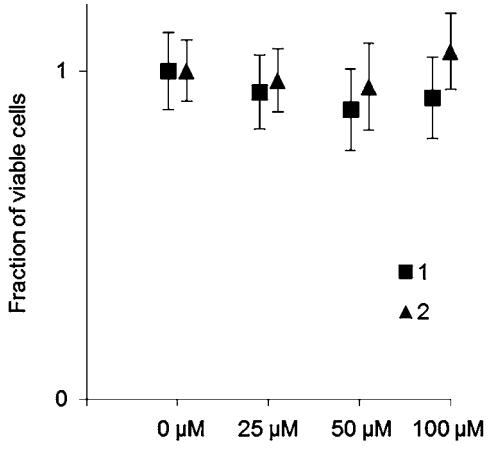

Figure 5. Viability of PPC-1 cells exposed to **1** (■) or to **2** (▲) as determined with PrestoBlue normalized to the control without added complex. Numbers of cells (~2.5 × 10^4 for the controls) were calculated by comparing the fluorescence intensities to a calibration curve. Each concentration was seeded in quadruplicate; error bars represent standard deviations.

band at 345 nm (ε = 3500 M^{-1} cm^{-1}) and tailing into the visible region (Figure 3), making dilute solutions light yellow.

Photolysis (λ_{irr} = 405 nm) of **1** in aqueous media or in acetonitrile led to changes in the IR and optical absorption spectra, as illustrated in Figures 2 and 3, respectively. Exhaustive photolysis in acetonitrile gave two ν_{CO} bands at 1937 and 1863 cm^{-1}. The IR spectral changes can be attributed to formation of the dicarbonyl solvento product $[Re(bpy)(CO)_2(sol)(thp)]^+$ (**2**) (sol = H_2O, CH_3CN). The optical spectrum of the product of exhaustive photolysis in water displayed bands at 290 and 405 nm. The shift of the MLCT band maximum from 345 to 405 nm and the shifts of the ν_{CO} bands to lower frequency are consistent with replacement of one CO with a more electron-donating solvento ligand. Additionally, analysis of the gaseous headspace by gas chromatography with thermal conductivity detection (GC-TCD)[12] revealed that the amount of CO generated by exhaustive photolysis of the aqueous solutions was approximately equal to the amount of **1** present. In this context, we conclude that 405 nm photolysis of **1** leads to dissociation of a single CO, in agreement with Ishitani and co-workers,[10b] who

dx.doi.org/10.1021/ja3084434 | J. Am. Chem. Soc. 2012, 134, 18197−18200

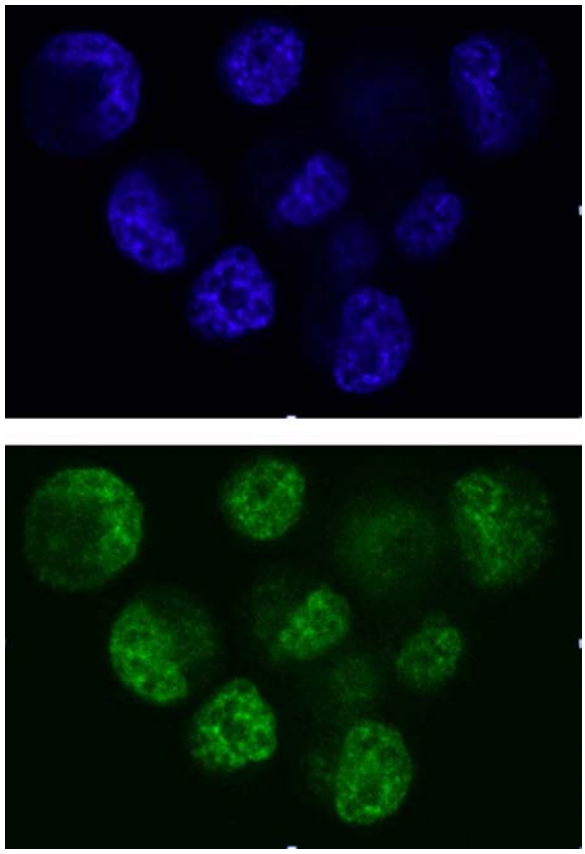

Figure 6. Confocal fluorescence microscopy images of PPC-1 cells that were incubated for 60 min with 50 μM **1**. The top image (in blue, λ_{em} = 465−495 nm) was collected with minimal photolysis from the 405 nm excitation source and indicates the incorporation of **1** into the cellular cytosol. The bottom image (in green, λ_{em} > 660 nm) was collected after 405 nm photolysis for 15 min and indicates the transformation of **1** to **2**.

showed that irradiation of the analogous *fac*-[Re(bpy)(CO)$_3$(P(OEt)$_3$)]$^+$ complex leads to stereospecific substitution of the CO trans to the phosphine (eq 1). Quantum yields for this photochemical process were determined in phosphate buffer solutions (10 mM, pH 7.4) using the changes in the optical spectra (see the SI for experimental details). For photolysis at 365 nm, a quantum yield of 0.21 ± 0.01 was determined; however, with 405 nm excitation, this dropped to 0.11.

Notably, **1** is also strongly luminescent in ambient-temperature aqueous solution with an emission band centered at 515 nm (Figure 4; see Figure S-1 in the SI for the excitation spectrum). This band can be assigned to phosphorescence from the triplet MLCT excited state, as seen for other *fac*-[Re(bpy)(CO)$_3$(PR$_3$)]$^+$ complexes.[10] More remarkable is the observation that the photoproduct **2** is also strongly luminactive in aqueous solutions with the emission maximum (λ_{max}^{em}) red-shifted to 585 nm. The quantum yields for these emissions were determined by using the emission from rhodamine B (Φ_{em} = 0.65)[13] as a comparative standard. In this manner, a Φ_{em} value of 0.18 ± 0.01 was measured for an aqueous solution of **1** ($CF_3SO_2^-$ salt) at ambient temperature with an excitation wavelength (λ_{ex}) of 365 nm. A roughly comparable value, Φ_{em} = 0.15, was measured at λ_{ex} = 405 nm. In the absence of a pure, well-characterized sample of **2**, an accurate determination of Φ_{em} was not made. However, given the strong luminescence behavior of the product solutions and the higher absorbance of **2** at λ_{ex} = 405 nm (Figure 4), we estimate the emission efficiency of **2** to be on the same order of magnitude but somewhat smaller than that of **1**.

Another notable feature of the emission behavior of **1** and **2** relevant to potential biological applications is the insensitivity of the emission intensities and lifetimes to the presence of air. The lifetimes of this emission were measured in aqueous media by laser flash photolysis techniques and found to be 405 ns for **1** and nearly the same (410 ns) for **2**. Notably, both lifetimes were independent of whether the solutions were aerated or deaerated.

A suitable photoCORM requires compatibility with physiological conditions. In this context, **1** is not only soluble and stable in aqueous media but also resistant to autoxidation. A solution of **1** in aerated phosphate buffer (10 mM, pH 7.4) at 37 °C showed no spectral changes over the course of 12 h when kept in the dark, thus indicating the long-term stability of **1** under such conditions.

The toxicities of **1** and **2** were probed by incubating cells from the human prostatic carcinoma cell line PPC-1 with varying concentrations of these species in the dark at 37 °C (5% CO_2). Solutions of **1** and **2** (1 mM each, $CF_3SO_2^-$salt) were prepared in phosphate-buffered saline (PBS, pH 7.2), and aliquots of these were added to wells containing PPC-1 cells (see the SI). Cell viability was determined using PrestoBlue, a fluorescent indicator of cell proliferation. Three concentrations of each complex (25, 50, and 100 μM) and a control (0 μM) were seeded in quadruplicate, and the cells were incubated at 37 °C (5% CO_2) for a period of ∼2 h. The PrestoBlue was then added to each well, and after incubation for 45 min, the fluorescence intensity at 590 nm (λ_{ex} = 560 nm) was measured. This was compared to a calibration curve to determine the number of viable cells. The results of this assay (Figure 5) demonstrated that over the course of a typical experiment, there was no immediate adverse effect from **1** or **2**, with greater than 88% cell viability for concentrations up to 100 μM. (See the SI for further comments regarding toxicity.)

The cellular uptake and photoreactivity of the photoCORM were probed by using the luminescence properties of **1** and **2** as in vitro markers, since the wavelength red-shifts upon CO loss. To test this multiplex-imaging methodology, adhered PPC-1 cells were incubated with 50 μM **1** at 37 °C for 60 min in the dark. The cells were rinsed several times with PBS to remove residual photoCORM in the medium, and then an aliquot of the cell suspension was mounted onto a microscope slide without fixing. Images were then immediately collected using an Olympus Fluoview 500 laser scanning fluorescence confocal microscope equipped with differential interference contrast optics, four photomultiplier tube detectors, and a 405 nm diode laser source for excitation. With the filter-based system, the luminescence between 465 and 495 nm should correspond to emission from **1**, while that at wavelengths >660 nm should primarily correspond to emission from **2**. However, since **1** is photolabile, it was important to capture and optimize each image quickly at low laser power to minimize CO loss during the acquisition. After such images were collected, the cells were exposed to increased power of the instrument's 405 nm diode laser (exact intensity unknown) to effect the photoreaction described by eq 1, and new images were then collected.

Figure 6 shows the results of these experiments. The top image (emission in the 465−495 nm window, shown in blue) clearly shows that **1** accumulated in the cytoplasm but did not appear to penetrate the nuclear envelope of PPC-1 cells. Upon

dx.doi.org/10.1021/ja3084434 | J. Am. Chem. Soc. 2012, 134, 18197−18200

photolysis with 405 nm light, there was a marked decrease in the emission intensity in the 465−495 nm window and strongly enhanced emission at the longer wavelengths. This correlates to photoinduced loss of **1** and generation of **2** within the cells. Although CO release was not directly observed, the transformations observed here were clearly consistent with intracellular CO release. Similar cellular uptake of a $(\eta^5\text{-}C_5H_5)Re(CO)_3$ derivative was recently demonstrated using the near-field technique known as photothermal-induced resonance.[14]

In summary, we have reported the synthesis of a biologically compatible photoCORM, *fac*-$[Re(bpy)(CO)_3(thp)](CF_3SO_3)$ that is water-soluble, air-stable, and nontoxic. Additionally, it is multifunctional, releasing CO upon irradiation while also serving as an imageable reporter to indicate the location where CO is being delivered on the cellular scale. The studies described here with live PPC-1 cells demonstrate its applicability and relative ease of use. This photoCORM has the potential to serve as a valuable tool for elucidating the poorly understood physiological role(s) of CO. Since the optical absorption properties of **1** are not ideal for in vivo applications because of the relatively low transmittance of shorter visible wavelengths in tissue,[15] we are exploring multiphoton excitation options[16] that may provide the opportunity to use longer-wavelength light sources for this purpose.

■ ASSOCIATED CONTENT

Ⓢ Supporting Information

Details regarding experimental procedures, further comments on toxicity, and crystallographic parameters. This material is available free of charge via the Internet at http://pubs.acs.org.

■ AUTHOR INFORMATION

Corresponding Author

ford@chem.ucsb.edu.

Notes

The authors declare no competing financial interest.

[†]First reported at the 243rd National Meeting of the American Chemical Society, San Diego, CA, March 2012; INOR-864.

■ ACKNOWLEDGMENTS

This work was supported by Grant CHE-1058794 to P.C.F. from the U.S. National Science Foundation (NSF) and by a fellowship to A.E.P. from the UCSB Partnership for International Research and Education in Electron Chemistry and Catalysis at Interfaces (NSF Grant OISE-0968399). A.P. was supported by the Institute for Collaborative Biotechnologies through Grant DAAD19-03-D-0004 from the U.S. Army Research Office. We thank Dr. Norbert Reich for cell culture facility use and Dr. Mary Raven for her aid with confocal microscopy. The confocal microscope was purchased on a NCRR Shared Instrumentation NIH Grant (#1S10RR017753-01).

■ REFERENCES

(1) Sjostrand, T. *Scand. J. Clin. Lab. Invest.* **1949**, *1*, 201.

(2) (a) Otterbein, L. E.; Zuckerbraun, B. S.; Haga, M.; Liu, F.; Song, R.; Usheva, A.; Stachulak, C.; Bodyak, N.; Smith, R. N.; Csizmadia, E.; Tyagi, S.; Akamatsu, Y.; Flavell, R. J.; Billiar, T. R.; Tzeng, E.; Bach, F. H.; Choi, A. M.; Soares, M. P. *Nat. Med.* **2003**, *9*, 183. (b) Wu, M. L.; Ho, Y. C.; Yet, S. F. *Antioxid. Redox Signaling* **2011**, *15*, 1835.

(3) (a) Katori, M.; Busuttil, R. W.; Kupiec-Weglinski, J. W. *Transplantation* **2002**, *74*, 905. (b) Neto, J. S.; Nakao, A.; Kimizuka, K.; Romanosky, A. J.; Stolz, D. B.; Uchiyama, T.; Nalesnik, M. A.; Otterbein, L. E.; Murase, N. *Am. J. Physiol.: Renal Physiol.* **2004**, *287*, F979. (c) Halilovic, A.; Patil, K. A.; Bellner, L.; Marrazzo, G.; Castellano, K.; Cullaro, G.; Dunn, M. W.; Schwartzman, M. L. *J. Cell Physiol.* **2011**, *226*, 1732.

(4) Fukuto, J. M.; Carrington, S. J.; Tantillo, D. J.; Harrison, J. G.; Ignarro, L. J.; Freeman, B. A.; Chen, A.; Wink, D. A. *Chem. Res. Toxicol.* **2012**, *25*, 769.

(5) Romao, C. C.; Blaettler, W. A.; Seixas, J. D.; Bernardes, G. J. L. *Chem. Soc. Rev.* **2012**, *41*, 3571.

(6) (a) Motterlini, R.; Clark, J. E.; Foresti, R.; Sarathchandra, P.; Mann, B. E.; Green, C. J. *Circ. Res.* **2002**, *90*, e17. (b) Johnson, T. R.; Clark, J. E.; Foresti, R.; Green, C. J.; Motterlini, R. *Angew. Chem., Int. Ed.* **2003**, *42*, 3722. (c) Motterlini, R.; Otterbein, L. E. *Nat. Rev. Drug Discovery* **2010**, *9*, 728.

(7) (a) Schatzschneider, U. *Inorg. Chim. Acta* **2011**, *374*, 19. (b) Rimmer, R. D.; Pierri, A. E.; Ford, P. C. *Coord. Chem. Rev.* **2012**, *256*, 1509.

(8) The term "caged" is commonly used for a bioactive compound that is released from its precursor by the absorption of light at the appropriate wavelength. See: Ciesienski, K. L.; Franz, K. J. *Angew. Chem., Int. Ed.* **2011**, *50*, 814.

(9) Kutal, C.; Weber, M. A.; Ferraudi, G.; Geiger, D. *Organometallics* **1985**, *4*, 2161.

(10) (a) Hori, H.; Koike, K.; Ishizuka, M.; Takeuchi, K.; Ibusuki, T.; Ishitani, O. *J. Organomet. Chem.* **1997**, *530*, 169. (b) Koike, K.; Okoshi, N.; Hori, H.; Takeuchi, K.; Ishitani, O.; Tsubaki, H.; Clark, I. P.; George, M. W.; Johnson, F. P. A.; Turner, J. J. *J. Am. Chem. Soc.* **2002**, *124*, 11448.

(11) Doud, M. D.; Grice, K. A.; Lilio, A. M.; Seu, C. S.; Kubiak, C. P. *Organometallics* **2012**, *31*, 779.

(12) Rimmer, R. D.; Richter, H.; Ford, P. C. *Inorg. Chem.* **2010**, *49*, 1180.

(13) Kubin, R. F.; Fletcher, A. N. *J. Lumin.* **1982**, *27*, 455.

(14) Policar, C.; Waern, J. B.; Plamont, M.-A.; Clède, S.; Mayet, C.; Prazeres, R.; Ortega, J.-M.; Vessières, A.; Dazzi, A. *Angew. Chem., Int. Ed.* **2011**, *50*, 860.

(15) (a) König, K. *J. Microsc.* **2000**, *200*, 83. (b) Smith, A. M.; Mancini, M. C.; Nie, S. *Nat. Nanotechnol.* **2009**, *4*, 710.

(16) (a) Garcia, J. V.; Yang, J.; Shen, D.; Yao, C.; Li, X.; Stucky, G. D.; Zhao, D.; Ford, P. C.; Zhang, F. *Small* **2012**, DOI: 10.1002/smll.201201213. (b) Garcia, J. V.; Zhang, F.; Ford, P. C. *Philos. Trans. R. Soc., A.* **2012**, in press.